Finite element analysis of tactile sensors made with screen printing technology

Julián Castellanos-Ramos[a], Rafael Navas-González[a], Estíbalitz Ochoteco[b] and F. Vidal-Verdú[a]
[a]Dept. of Electronics, University of Malaga, Málaga, Spain, julian@elca.uma.es;
[b]Dept. of New Materials, CIDETEC, San Sebastián, Spain, EOchoteco@cidetec.es

ABSTRACT

Tactile sensors have increasing presence in different applications, especially in assistive robotics or medicine and rehabilitation. They are basically an array of force sensors (tactels) and they are intended to emulate the human skin. Large sensors must be implemented with large area oriented technologies like screen printing. The authors have proposed and made some piezoresistive sensors with this technology. They consist of a few layers of conductive tracks to implement the electrodes and elastomers to insulate them, on a polymer substrate. Another conductive sheet is placed atop the obtained structure. Pressure distribution in the interface between this conductive sheet and the electrodes has a direct impact on the sensor performance. The mechanical behavior of the layered topology with conductive tracks, elastomers and polymers must be studied. For instance, the authors have observed experimentally the existence of pressure thresholds in the response of their sensors. Finite element simulations with COMSOL explain the reason for such thresholds as well as the dependence of the pressure distribution profile on the properties of the materials and the geometry of the tactel. This paper presents results from these simulations and the main conclusions that can be obtained from them related to the design of the sensor.

Keywords: Tactile sensors based on conductive polymers, sensors fabricated with screen printing technology.

1. INTRODUCTION

Tactile sensors are basically arrays of force sensors that provide pressure maps. Most of them are based on piezoresistive [1][2][3][4] or capacitive principles [5][6][7]. Signal conditioning of capacitive sensors involves the use of an alternating voltage or current, and special care has to be taken with parasitic capacitors, so it is quite complex and is usually implemented on chip or close to the raw sensor. Piezoresistive tactile sensors can be fabricated in a quite simple way and their electronics are also simpler than that for capacitive sensors, so they are more common. Different technologies have been applied to fabricate these sensors. Small size and high spatial resolution sensors are obtained with Micro Electro-Mechanical Systems (MEMS) on silicon [2][3][5]. However the fragility of silicon limits their practical use. Other sensors are developed with MEMS on polymers [1][4], so they are flexible and can withstand larger forces than those based on silicon. Many large area sensors have been built by placing a sheet of material with piezoresistive properties atop of an array of electrodes on a Printed Circuit Board (PCB) [8]. Others use Force Sensing Resistors soldered on a PCB [9]. These sensors have limited flexibility and the cost of the assembly can be high in the latter case. A better option to develop a flexible and low cost sensor is the use of a screen printing technology. A sensor based on this technology is commercialized by Tekscan [10]. The authors have proposed and developed another sensor made with this technology. This sensor is composed of a few layers of conductive and insulated materials on a plastic background and another plastic sheet that is covered by a conductive polymer atop [8]. A few sensors have been fabricated to prove the viability of the proposal. Nevertheless, a deeper study of the implications of the choice of different values for some material properties and of the size and shape of the different layers was still pending. This paper shows results and discussions obtained mainly from Finite Element Analysis (FEA). This procedure is quite common in the design of tactile sensors able to measure shear forces. In the case of the sensor we propose, FEA allows obtaining information to design the sensor with an optimum sensitivity, and to control the range and threshold. In the following, the technology to build the sensors is described and two proposals for the fabrication of a tactel (single sensing unit on a tactile sensor array) of the tactile sensor are presented together with analysis based on simple calculations and FEA simulations.

2. TECHNOLOGY

Screen printing technology is a low cost thick film process that has been widely used in artistic applications and more recently in the production of electronic circuits and sensors. In the 80s the process was adapted to the production of different types of sensors [11][12], making their commercialization much easier. This was due to the multiple advantages that the technology offers including reduced expense, flexibility, process automation, reproducibility and wide selection of materials. A huge number of successful devices have been built using this technique [13].

The process of screen printing is rapid and simple. It consists of squeezing an ink or paste through a patterned screen onto a substrate held on the reverse of the screen. Successive layers can be deposited by this procedure and patterns can be replicated onto the same screen to enhance production speed. The substrate needs to be an inert material, most commonly PVC, polycarbonate, polyester or ceramic, although nitrocellulose and glass fiber are also employed. Each layer is deposited through the corresponding mask providing a specific pattern. These masks are prepared by a photolithographic technique with photosensitive gels and nylon, polyester or stainless steel meshes.

There are mainly two types of pastes that can be used in screen printed electrode (SPE) production: conductive or dielectric inks. The conductive inks give rise to the formation of conductive tracks on the electrodes. They are based on an organic binder where gold, silver, platinum or graphite are dispersed at high loads as conducting fillers. Recently water based inks have also been employed [14]. Dielectric inks are often based on polymers or ceramics and they form the encapsulating layer of the sensor, delimiting the working area and electric contacts.

2.1 Materials

Ethylenedioxythiophene (EDOT) monomer (99%), ammonium peroxydisulphate, and poly(styrene sulfonate, sodium salt) (PSS) were purchased from Sigma-Aldrich Chemicals S.A. Silver paste was purchased from Dupont. Dielectric acrylate elastomeric inks were purchased from Twintec.

2.2 Electrode array fabrication

The screen-printing fabrication procedure has been used for the fabrication of conducting and non-conducting tracks on a PET (polyethylene terephthalate) flexible plastic support. The conducting paths act as electrodes, enabling the electrical connection of the different sensor elements. The elastomeric non-conducting paths are deposited to insulate conducting paths, and they allow the working pressure range of the sensor to be controlled. The configuration and distribution of the conducting paths determines the size of each sensor element and their geometry. The different geometries studied will be later described in detail. The technology design rules are shown in Table 1.

2.3 Conducting ink preparation

A conducting polymer dispersion was used as conducting ink for its application on a flexible plastic sheet. Poly(3,4-ethylenedioxythiophene) (PEDOT) was chosen as conducting raw material, and aqueous dispersions of this polymer were prepared to obtain conducting inks. PEDOT aqueous dispersions were prepared by using an Ultrasonic Processor (model UP 400 S from Dr. Hielscher GmbH) during the synthesis. As an example, ethylenedioxythiophene (1 ml, 9.4 mmol) and 3.5 g of poly(styrene sulfonate, sodium salt) were dissolved in 100 ml of distilled water. To this mixture, an equimolar amount of ammonium peroxydisulphate (6.58 g, 28.8 mmol) dissolved in 50 ml of water was added dropwise over a period of 4 min. After 1 h of reaction under ultrasonic irradiation a dark blue PEDOT aqueous dispersion was obtained.

2.4 Flexible conducting sheets preparation

Conducting flexible sheets were prepared placing a PET (polyethyleneterephtalate, 5 x 5 cm2 in surface, 70 μm in thickness) plastic sheet on a spin coater. 50 μl of conducting polymer ink were dispensed on it and it was rotated at 1,500 rpm. After 1 min, it was stopped and left drying at room temperature. A thin conducting film was created on the plastic sheet, giving a conducting flexible plastic sheet.

A key issue of the so obtained conductive plastic film is the microscopic roughness with an average grain size of 50nm because the working principle of the sensor is the variation of the effective area of contact at microscopic level and the change of the conductance as a consequence of it [15].

Table 1. Technology design rules.

Minimum diameter (mm)	Minimum annular ring (mm)	Minimum width (mm)	Minimum clearance (mm)	Minimum layer thickness (mm)
0.1	0.1	0.1	0.1	0.01
				

3. ANALYSIS AND MODELLING OF THE PROPOSED DESIGNS

As said above, the sensitivity of a tactile sensor made with the described technology depends on the microscopic roughness of the conducting sheet in the side that makes contact with the electrodes. The modelling of the associated behavior at this micro or even nano scale is beyond the scope of this paper. We are interested in knowing how the mechanical properties of the materials and the geometry of the tactel affect the global behavior, so this model is not necessary. We will focus on the pressure at the conductive sheet-electrodes interface instead, because we know that the higher this pressure is the larger the sensor output is. Specifically, we propose two alternatives to design a single tactel and we analyze and discuss their performance through simple calculations and mainly with simulations of their mechanical behavior using the finite elements analysis software COMSOL 3.4. In particular, the structural mechanics module is used to simulate a cross section of the tactel. Every tactel is composed by five layers which are from bottom to top: the substrate, the outer electrode, the insulator, the inner electrode, and the conductive sheet (see Figure 1(a) and Figure 3 where the substrate layer is not shown in the figures). The value of the parameters of the materials we used in the simulations is shown in Table 2. In addition, the size of the tactel is 2.54 mm and the distance between conductive tracks is 0.2 mm.

Table 2. Young's modulus and Poisson's ratio values.

Layer	Young's modulus (E)	Poisson's ratio (nu)
conductive sheet	2.42 GPa	0.37
insulator	3 MPa	0.48
electrode	83 GPa	0.37

3.1 First proposal

Figure 1 shows a quite straightforward implementation of a tactel with the above described technology. It is named SME1 hereafter. Its shape and dimensions are shown in Figure 1(a), while Figure 1(b) shows the deformation and displacement along the y axis of its layers for a uniform applied pressure of 60 PSI. Note that the whole area of the inner electrode is in contact with the conducting sheet while it is not the case of the outer electrode. Figure 1(c) shows the contact pressure on the left side of the outer electrode for an applied pressure on the conducting sheet between 0 and 60 PSI. When the pressure increases, the conducting sheet bends until it makes contact with the external electrode. No output is registered from the sensor before this contact is made, so there is a threshold in the response. This was observed experimentally in a first prototype of the sensor [8]. Figure 1(d) shows the measured output of this prototype with a threshold of 15PSI. After the initial contact is established, the contact area between the conducting sheet and the external electrode increases with the applied pressure. Note that this increase of the macroscopic area of contact is added to the increment of the microscopic area of contact mentioned above.

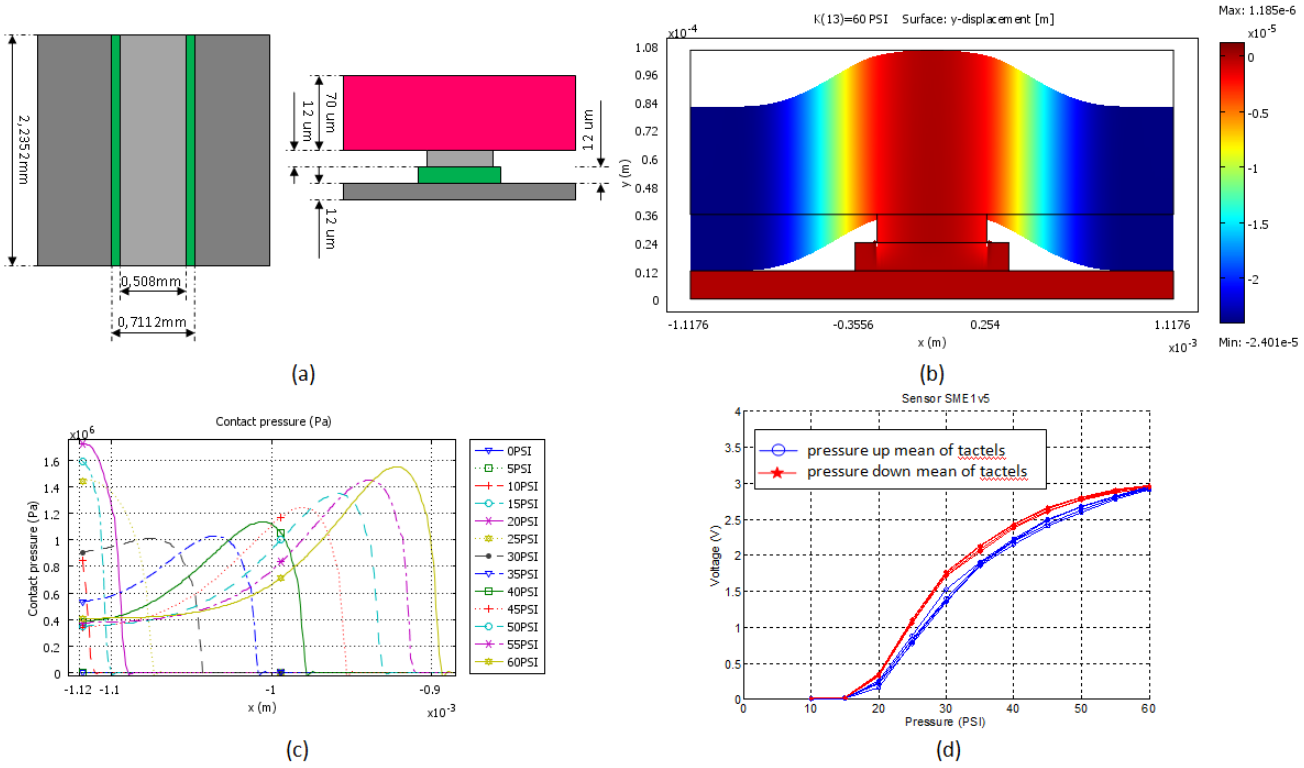

Figure 1. Shape and dimensions of tactel SME1 (the conductive sheet layer has been removed in the top view) (a), simulation output for a uniform pressure: y-displacement for 60 PSI (b), contact pressure in the left side of the external electrode (c); and an experimental measure of a prototype (d).

It is possible to explore the behaviour of the sensor if we assume that the measured pressure threshold of 15PSI can be translated into an equivalent minimum contact area given by the point where the 15 PSI curve crosses the x axis in Figure 1(c). Figure 2 shows the external pressure required for this minimum area is reached when the thickness and compliance of the conductive sheet are changed. It can be observed that the pressure threshold increases if the Young's modulus of the conductive sheet (E_{pedot}) increases. Moreover, if the thickness of the conductive sheet decreases, the pressure threshold also decreases.

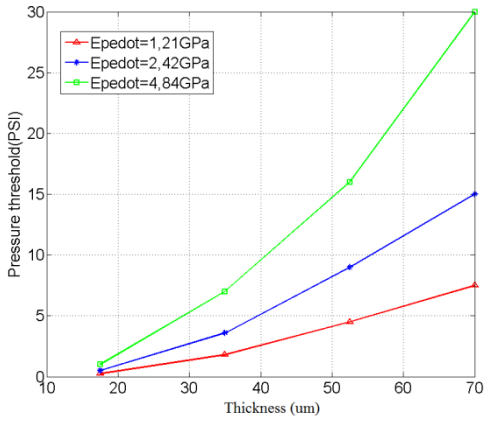

Figure 2. Variation of the pressure threshold with the conductive sheet thickness and E_{pedot}.

Although the design described in this section is simple, the observed threshold limits its use. Moreover, if we press with a rigid flat object against the tactel, no reading at all is registered from the sensor for any applied pressure because the contact between the conductive sheet and the outer electrode is never established. The following section shows a proposal that overcomes these drawbacks

3.2 Second proposal

Figure 3 shows the second proposal for the design of a tactel. It will be named SME1v2 in the following. Similar conditions for both interfaces of the conductive sheet with the inner and outer electrodes are established this time. First, the area of both electrodes is the same, which improves the sensitivity of similar sensors made on printed circuit boards [8]. Second, both are placed at the same height to achieve both electrodes are in contact with the conductive sheet at very low pressures and avoid a pressure threshold in the sensor response.

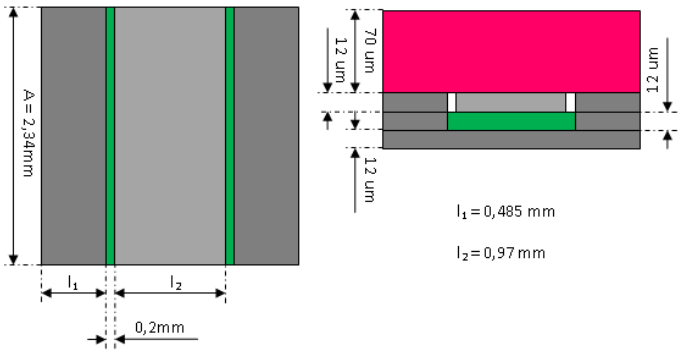

Figure 3. Dimensions of tactel SME1v2.

Figure 4 shows the output of the FEA simulation when a uniform pressure is applied on the surface of the sensor. Note that the macroscopic contact area between the conductive sheet and the internal and external electrodes is the same and approximately constant for all the range of applied pressure. Moreover, the contact pressure in the interface between the conductive sheet and both electrodes is the same. Actually, this contact pressure is also quite uniform along the interface except in areas close to the borders.

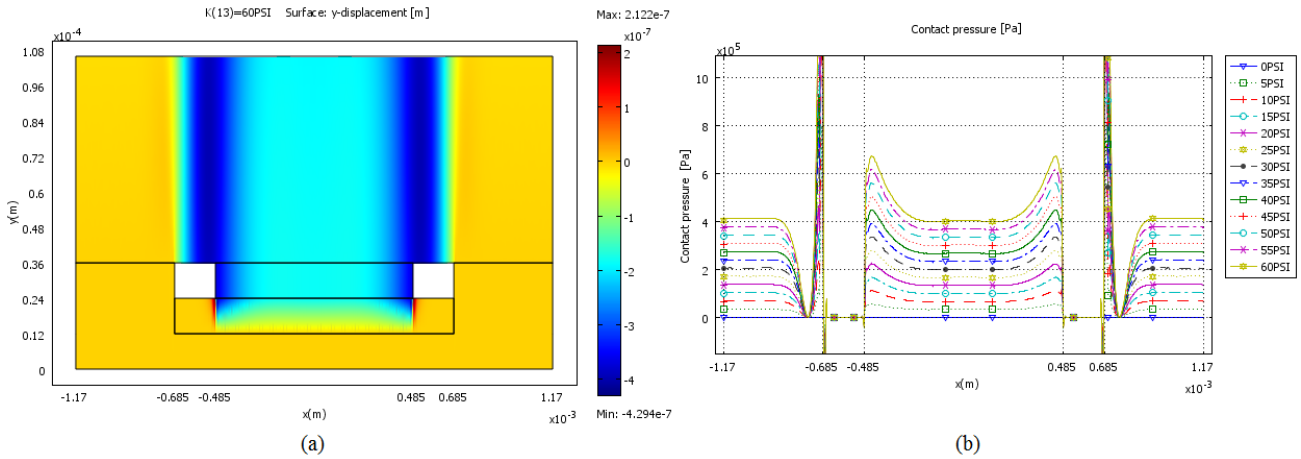

Figure 4. Simulation output for SME1v2 with a uniform pressure applied: y-displacement for 60 PSI (a) and contact pressure between conductive sheet layer and electrodes (b).

A very different behaviour is observed if the pressure against the sensor is not supposed uniform. For instance, if a flat rigid object presses the sensor the pressure along the interface between this object and the sensor is not uniform. Figure 5 shows the displacement along axis y and the contact pressure at interface with the electrodes for different values of the pressure applied onto a flat rigid object. Note that the contact pressure in the interface with the inner electrodes is much lower than that in the interface with the outer electrode. Remember the tactel is actually a force sensing resistor, so a simple electrical model of it consists of the connection in series of the resistances associated to the interfaces with the electrodes plus that associated to the path between them. If the resistance associated to one of the electrodes is high, the total resistance will be also high and the sensitivity of the sensor will be small. This is the case observed in Figure 5(b), where the resistance associated to the inner electrode is high. On the contrary, the symmetry of Figure 4(b) means that both resistances are balanced approximately.

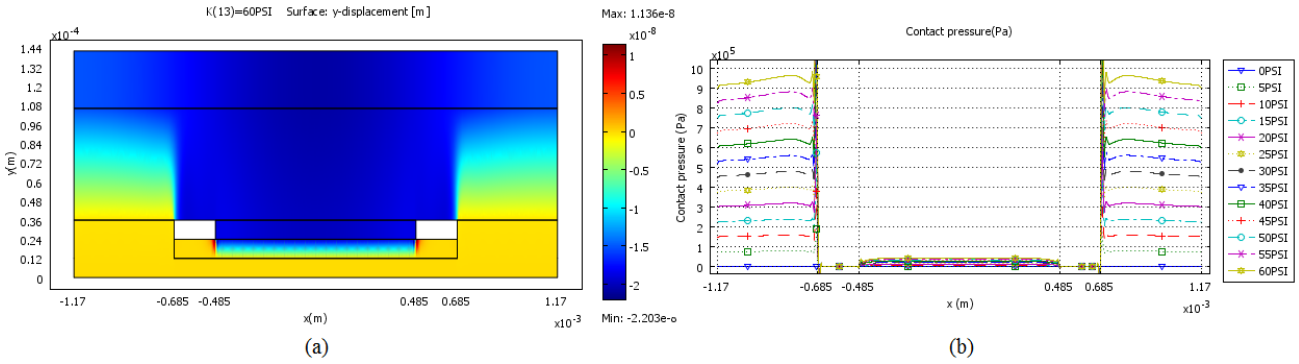

Figure 5. Simulation output for SME1v2 with a uniform pressure applied through a flat rigid object: y-displacement for 60 PSI (a) and contact pressure between conductive sheet layer and electrodes (b).

In order to obtain a response similar to that in Figure 4(b) for this stimulus, we have to set the proper values for the parameters of the materials and the geometry of the tactel. This is a difficult task if it is only based on simulations. However, a simple model can be used to obtain them in a first approximation. Figure 6(a) shows the pressure distribution along axis y for the same experiment of Figure 5. Note that two quite uniform zones can be clearly distinguished in the graph and are associated to the inner and outer electrodes. Each zone can be modeled as a stacked structure of layers with area A_{layer}, thickness l_{layer} and elastic constant given by:

$$K_{layer} = \frac{E_{layer} \cdot A_{layer}}{l_{layer}} \tag{1}$$

where E_{layer} is the Young's modulus of the layer. Therefore, the simple model depicted in Figure 6(b) can be used to analyze the behavior and obtain guidelines for the design of the tactel.

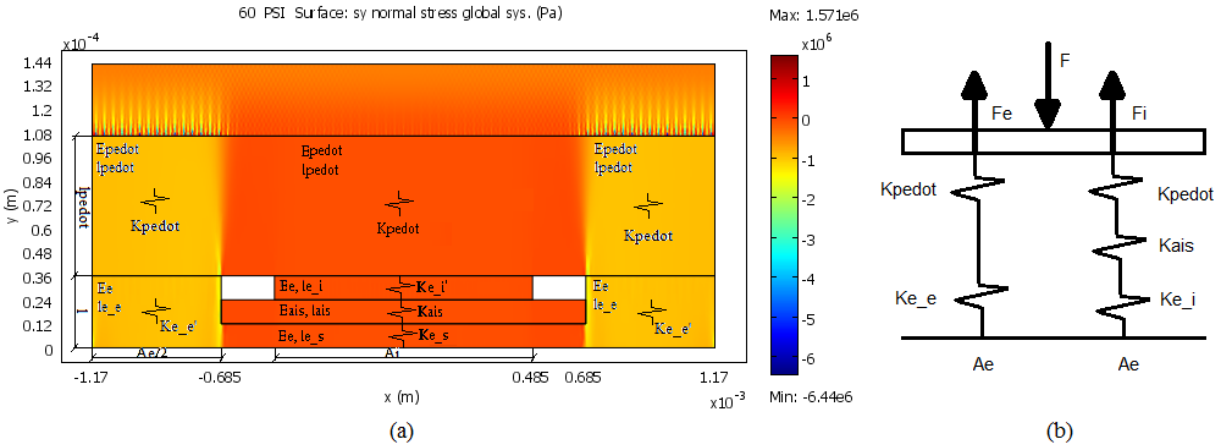

Figure 6. Simulation output for SME1v2 with a uniform pressure applied through a flat rigid object: sy global stress for 60 PSI (a); and two springs simplified model (b).

For the sake of clarity, we define the parallel operator as:

$$(a \parallel b) = \frac{a \cdot b}{a + b} \tag{2}$$

Having into account that $F = -(F_i + F_e)$ in Figure 6(b), we can write the following expressions for the interfaces with the electrodes:

$$F_i = -\frac{(K_{pedot} \parallel K_{ais} \parallel K_{e\_i})}{K_{eq}} \cdot F = -\frac{(K_{ais} \parallel K_{e\_i})}{K_{eq}} \cdot F \cdot \alpha \tag{3}$$

$$F_e = -\frac{(K_{pedot} \parallel K_{e\_e})}{K_{eq}} \cdot F \tag{4}$$

where F is the global force exerted on the tactel, F_i is the reaction force in the internal electrode, F_e is the reaction force in the external electrode, $\alpha = \frac{K_{pedot}}{K_{pedot} + (K_{ais} \parallel K_{e\_i})} \in [0,1]$, and $K_{eq} = (K_{pedot} \parallel K_{ais} \parallel K_{e\_i}) + (K_{pedot} \parallel K_{e\_e})$ is the equivalent elastic constant of the whole tactel.

This simple model explains the behavior observed in Figure 5. Table 3 shows the values of the elastic constants obtained from the Young's modulus of the materials (see Table 2) and the geometry of the tactel (see Figure 3, Figure 6(a) and expression (1)).

Table 3. Model parameter expressions and values.

Parameter	Expression	Value
K_{pedot}	$\frac{E_{pedot} \cdot A_e}{l_{pedot}}$	$34{,}57 \cdot 10^{12} \cdot A_e$ N/m
K_{e_e}	$\frac{E_e \cdot A_e}{3 \cdot l}$	$2305{,}56 \cdot 10^{12} \cdot A_e$ N/m
K_{e_i}	$\frac{E_e \cdot A_e}{2 \cdot l}$	$3458{,}33 \cdot 10^{12} \cdot A_e$ N/m
K_{ais}	$\frac{E_{ais} \cdot A_e}{l}$	$0{,}25 \cdot 10^{12} \cdot A_e$ N/m

We conclude from Table 3 that $K_{e\_e} \approx K_{e\_i}$, $K_{e\_e} \approx 100 \cdot K_{pedot}$ and $K_{pedot} \gg K_{ais}$, so (3) and (4) can be simplified as:

$$F_i \approx -\frac{K_{ais}}{K_{eq}} \cdot F \tag{5}$$

$$F_e \approx -\frac{K_{pedot}}{K_{eq}} \cdot F \tag{6}$$

and finally we obtain that $F_e \gg F_i$ as Figure 5 illustrates.

To obtain a behavior similar to that in Figure 4, the contact pressure at the interface of both electrodes must be the same. Since the areas of the electrodes are equal, this is achieved for $F_e = F_i = F/2$.

$$F_e = F_i \Rightarrow (K_{pedot} \parallel K_{e\_e}) = (K_{pedot} \parallel K_{e\_i} \parallel K_{ais}) \Rightarrow K_{e\_e} = \frac{K_{e\_i} \cdot K_{ais}}{K_{e\_i} \cdot K_{ais}} \tag{7}$$

From the expressions of the elastic constants in Table 3 and (7) we can conclude that the Young's modulus of the insulator (E_{ais}) and the electrodes (E_e) must be equal. This is observed in Figure 7, where the output of a simulation for an applied pressure of 60PSI is shown. Note that the closer E_{ais} and E_e are, the closer the contact pressures at the interface of both electrodes are.

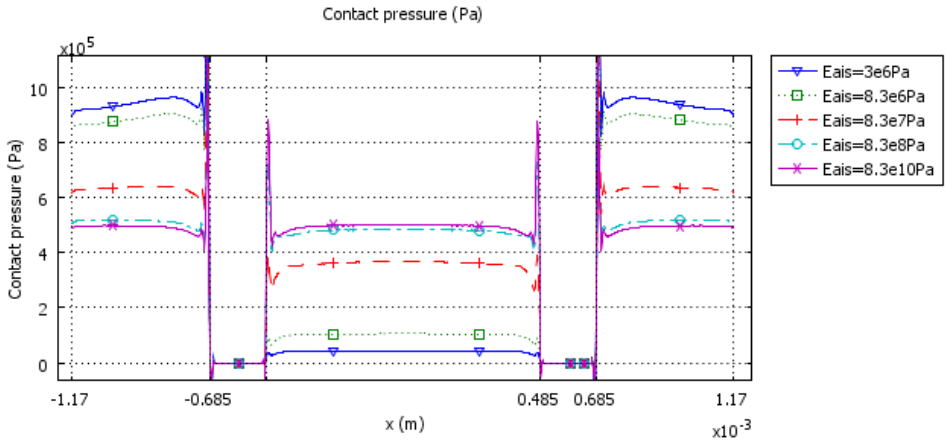

Figure 7. Simulation output for SME1v2 with a uniform 60 PSI pressure applied through a flat rigid object: contact pressure for different values of E_{ais}.

A similar result can be obtained with different combinations of the elastic constants. For instance, for $K_{e\_e} \approx K_{e\_i}$, $K_{ais} > K_{pedot}$ and $K_{e\_e} \gg K_{ais}$ we can write $K_{eq} = (K_{pedot} /\!/ K_{ais} /\!/ K_{e_i}) + (K_{pedot} /\!/ K_{e\_e}) \lesssim 2 \cdot K_{pedot}$ and (4) reduces to $F_e \gtrsim -\frac{F}{2}$.

In addition, $F_i \lesssim -\frac{(K_{ais} /\!/ K_{e\_i})}{2 \cdot K_{pedot}} \cdot F \cdot \frac{K_{pedot}}{K_{pedot} + (K_{ais} /\!/ K_{e\_i})}$ and then (3) is simplified as $F_i \lesssim -\frac{F}{2}$.

The condition $K_{ais} > K_{pedot}$ can be expressed as $\frac{E_{pedot}}{l_{pedot}} < \frac{E_{ais}}{l}$. Hence we can fulfill it by choosing the Young's modulus and the thickness of both (insulator and conductive sheet) layers properly and multiple solutions can be reached. For instance, Figure 8 shows the result of a simulation for a given geometry of the tactel (l_{pedot} and l) and $E_{ais} = E_{pedot}$ is between 3MPa and 2.42GPa (then $K_{ais} \approx 6 \cdot K_{pedot}$). The contact pressure is very similar in both electrodes for any value of E_{ais}.

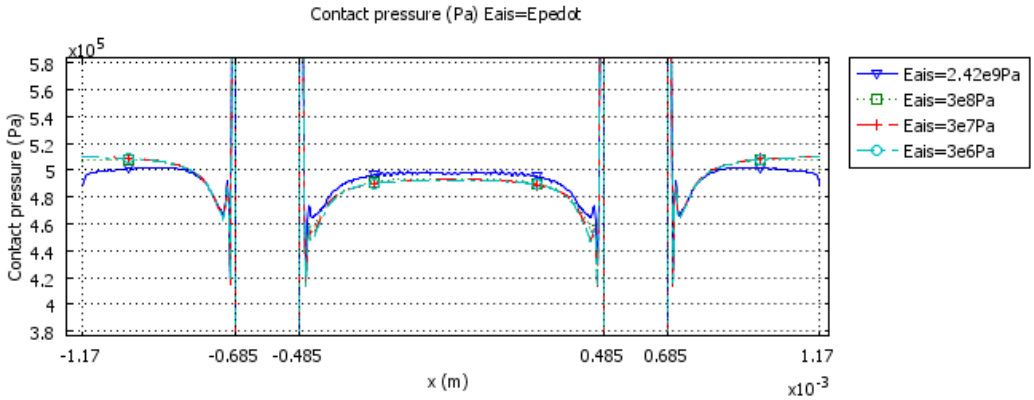

Figure 8. Simulation output for SME1v2 with a uniform 60 PSI pressure applied through a flat rigid object: contact pressure for different values of E_{ais} with $E_{pedot} = E_{ais}$.

CONCLUSIONS

This paper presents proposals to design a single tactel of a tactile sensor. Although they look for simplicity to lower the cost, the obtained layered structure is actually complex and many parameters have influence on the sensor response. Regarding the simplest structure, we measured a threshold experimentally that is explained from FEA simulations in this paper. The main conclusion is that the top conductive layer must be very compliant to reduce the threshold. Therefore the thinner it is and the smaller its Young's modulus is, the smaller the threshold is. Nevertheless, the asymmetry of the tactel is behind the existence of this threshold. Therefore we propose a new design where the areas of both electrodes are equal and they are placed at the same height to make contact with the conductive sheet for very low values of the pressure exerted against the sensor. We observe this early contact in our simulations and also a balanced response of the interfaces between the conductive sheet and both electrodes. If the contact area or the pressure at the interface with one electrode is much smaller in one electrode than in the other, the high resistance associated to the former will dominate the global performance of the sensor. Another important conclusion of the paper is that this balanced behaviour depends on the properties of the object that is in contact with the sensor. Most common situations involve contact with rigid objects. Our analysis and simulations show that a very unbalanced behaviour is observed even in the improved proposal if we press the sensor with a rigid object. In this case multiple combinations can be made to achieve a balanced response. Some are shown in the paper, where FEA simulations support them and a simplified model is also used to assist in the finding of these possible solutions.

ACKNOWLEDGMENTS

This work has been funded by the Spanish Government under contract TEC2009-14446.

REFERENCES

[1] Engel, J., Chen, N., Tucker, C., Liu, C., Kim, S.H. and Jones, D., "Flexible multimodal tactile sensing system for object identification," Proceedings of the IEEE Sensors Exco Daegu Korea, 563–566 (2006).
[2] Kane, BJ., Cutkosky, MR. and Kovacs, GTA., "A traction stress sensor array for use in high-resolution robotic tactile imaging," Electromech Syst 9(4), 425–434 (2000).
[3] Mei, T., Li, WJ., Ge, Y., Chen, Y., Ni, L. and Chan, MH. "An integrated MEMS three-dimensional tactile sensor with large force range," Sens Actuators 80, 155–162 (2000).
[4] Kim, K., Lee, KR., Lee, DS., Cho, N., Kim, WH., Park, K., Park, H., Kim, Y., Park, Y. and Kim, J. "A silicon-based flexible tactile sensor for ubiquitous robot companion applications," J Phys Conf Ser 34, 399–403 (2006).
[5] Salo, T., Vancura, T., Brand, O. and Baltes, H., "CMOS-Based Sealed Membranes for Medical Tactile Sensor Arrays," IEEE MEMS, 590-593 (2003).
[6] Leineweber, M., Pelz, G., Schmidt, M., Kappert, H. and Zimmer, G., "New tactile sensor chip with silicone rubber cover," Sens Actuators 84, 236–245 (2000).
[7] Paschen, U., Leineweber, M., Arnelung, J., Schmidt, M. and Zammer, G., "A novel tactile sensor for heavy-load applications based on an integrated capacitive pressure sensor," Sens Actuators 68, 294–298 (1998).
[8] Castellanos-Ramos, J., Navas-Gonzalez, R., Macicior, H., Sikora, T., Ochoteco, E. and Vidal-Verdú, F., "Tactile sensors based on conductive polymers," Microsystem Technologies 16(5), 765-776 (2010).
[9] Vidal-Verdú, F., Barquero, M.J., Serón, J. and García-Cerezo, A, "Large area smart tactile sensor for rescue robot," Proc. of IEEE Int. Workshop on Robotic and Sensor Environments ROSE09, 6–10 (2009).
[10] www.tekscan.com
[11] Baumbach, P. L., UK Patent number 2 073891, (1981).
[12] Liu, C. C., US Patent number 4 655, (1987).
[13] Zhang, X.E., "Screen printing methods for biosensor production," Biosensors 2nd edition ed. J. Cooper and T. Cass Eds.: Oxford University Press, 41-58 (2004).

[14] Crouch, E., Cowell, D. C., Hoskins, S., Pittson, R. W. and Hart, J. P., "A novel, disposable, screen-printed amperometric biosensor for glucose in serum fabricated using a water-based carbon ink," Biosensors and Bioelectronics vol. 21, 712-718 (2005).
[15] Ochoteco, E., Pomposo, JA., Sikora, T., Vidal, F., Martinez, F., Obieta, G. and Grande, H., "All-plastic distributed pressure sensors: taylormade performance by electroactive materials design," Microsystem Technologies 14(8), 1089–1097 (2008).